

# Intermittency in the relative separations of tracers and of heavy particles in turbulent flows

L. Biferale<sup>1</sup>, A. S. Lanotte<sup>2</sup>, R. Scatamacchia<sup>1,3</sup>,  
and F. Toschi<sup>3,4,5</sup>

<sup>1</sup>Department of Physics and INFN, Univ. of Tor Vergata,  
Via della Ricerca Scientifica 1, 00133 Rome, Italy

<sup>2</sup> CNR-ISAC and INFN- Sez. Lecce, Str. Prov. Lecce-Monteroni, 73100 Lecce, Italy

<sup>3</sup>Department of Physics, Eindhoven Univ. of Technology, 5600 MB Eindhoven, The Netherlands

<sup>4</sup>Department of Mathematics and Computer Science, Eindhoven Univ. of Technology,  
5600 MB Eindhoven, The Netherlands

<sup>5</sup> CNR-IAC, Via dei Taurini 19, 00185 Rome, Italy

(Accepted for publication in this finale form (postprint version) on J. Fluid Mech. **757**, 550 (2014))

Results from Direct Numerical Simulations of particle relative dispersion in three dimensional homogeneous and isotropic turbulence at Reynolds number  $Re_\lambda \sim 300$  are presented. We study point-like passive tracers and heavy particles, at Stokes number  $St = 0.6, 1$  and  $5$ . Particles are emitted from localised sources, in bunches of thousands, periodically in time, allowing to reach an unprecedented statistical accuracy, with a total number of events for two-point observables of the order of  $10^{11}$ .

The right tail of the probability density function for tracers develops a clear deviation from Richardson's self-similar prediction, pointing to the intermittent nature of the dispersion process. In our numerical experiment, such deviations are manifest once the probability to measure an event becomes of the order of -or rarer than- one part over one million, hence the crucial importance of a large dataset.

The role of finite-Reynolds effects and the related fluctuations when pair separations cross the boundary between viscous and inertial range scales are discussed. An asymptotic prediction based on the multifractal theory for inertial range intermittency and valid for large Reynolds numbers is found to agree with the data better than the Richardson theory. The agreement is improved when considering heavy particles, whose inertia filters out viscous scale fluctuations. By using the exit-time statistics we also show that events associated to pairs experiencing unusually slow inertial range separations have a non self-similar probability distribution function.

**Key words:** intermittency, multiphase and particle-laden flows, turbulent mixing

## 1. Introduction

Dispersion of particles in stochastic and turbulent flows is a key fundamental problem (Monin & Yaglom 1975) with applications in a huge number of disciplines going from atmospheric and ocean sciences (Bennett 1984; Lacorata et al. 2008; Ollittraut et al. 2005; Poulain & Zambianchi 2007; LaCasce 2010), to environmental sciences (Csanady 1973),

chemical engineering and astrophysics (Baldyga & Bourne 1999; Lepreti et al. 2012). At high Reynolds numbers, molecular diffusion makes a negligible contribution to spatial transport, and so turbulence dominates not only the transport of momentum, but also that of temperature, humidity, salinity and of any chemical species or concentration field. Mixing can be approached from an Eulerian point of view, studying the spatial and temporal evolution of a concentration field (Dimotakis 2005), and also by using a Lagrangian approach in terms of the relative dispersion of pairs of particles (Sawford 2001; Falkovich et al. 2001; Salazar & Collins 2009). Notwithstanding the enormous literature on the topic, a stochastic model for particle trajectories in turbulent flows whose basic assumptions are fully justified is yet to come (Thomson 1990; Borgas & Sawford 1994; Kurbanmuradov 1997; Borgas & Yeung 2004; Pagnini 2008). The modeling of pair dispersion for tracers was pioneered in Richardson (1926), where a *locality assumption* was introduced, see also Benzi (2011) for a recent historical review. In a modern language, Richardson’s approach is built up in analogy with diffusion, replacing molecular fluctuations with turbulent fluctuations, acting differently at different scales. Hence, in a turbulent flow, diffusivity is enhanced because the instantaneous separation rate depends on the local turbulent conditions encountered by pairs along their path:

$$\frac{d\langle r^2 \rangle}{dt} = D(r), \quad r_0 \ll r \ll L, \quad (1.1)$$

where  $r(t)$  is the amplitude of the separation vector between the two particles,  $\mathbf{r}(t) = \mathbf{X}_1(t) - \mathbf{X}_2(t)$ , and  $D(r)$  is a scalar eddy-diffusivity. For the eddy-diffusivity approach to be valid, separations  $r$  have to be chosen larger than the initial ones,  $r_0$ , and smaller than the integral scale of the flow,  $L$ . Moreover, time lags have to be large enough, so that the memory of the initial separation is lost.

In the light of Kolmogorov 1941 theory, (see Frisch (1995)), the scalar eddy-diffusivity can be modeled as follows:

$$D(r) \propto \tau(r, t) \langle (\delta_r u)^2 \rangle \sim k_0 \epsilon^{1/3} r^{4/3}, \quad (1.2)$$

where  $\delta_r u$  is the Eulerian longitudinal velocity difference along the direction of particle separation  $\mathbf{r}$ ,  $\delta_r u(\mathbf{r}(t), t) = \hat{\mathbf{r}} \cdot (\mathbf{u}(\mathbf{X}_1(t), t) - \mathbf{u}(\mathbf{X}_2(t), t))$ ,  $k_0$  is a dimensionless constant, and  $\epsilon$  is the rate of kinetic energy dissipation in the flow. In the above equation,  $\tau(r, t)$  is the correlation time of the Lagrangian velocity differences at scale  $\mathbf{r}$ ,

$$\tau(r, t) = \frac{2}{\langle [\delta_r u(\mathbf{r}(t), t)]^2 \rangle} \int_0^t \langle \delta_r \mathbf{u}(\mathbf{r}(t), t) \cdot \delta_r \mathbf{u}(\mathbf{r}(s), s) \rangle ds. \quad (1.3)$$

In the inertial range of scales, by dimensional considerations, we can write  $\tau(r) \simeq \epsilon^{-1/3} r^{2/3}$ , and  $\langle (\delta_r u)^2 \rangle \simeq (\epsilon r)^{2/3}$ , from which the celebrated Richardson’s 4/3 law of eqn. (1.2) follows. As a consequence, eqn. (1.1) predicts a super-diffusive growth for the particle separation:

$$\langle r^2(t) \rangle \simeq \epsilon t^3, \quad (1.4)$$

and the dependence on the initial conditions is quickly forgotten. In fact, when released into a fluid flow, tracer pairs separate ballistically at short time lags, *à la* Batchelor (Batchelor 1950), keeping memory of their initial longitudinal velocity difference,  $\langle r^2(t) \rangle \simeq (\langle r_0^2 \rangle + C(\epsilon r_0)^{2/3} t^2)$ , up to time lags of the order of  $t_B(r_0) \sim (r_0^2/\epsilon)^{1/3}$ . Only later on, Richardson’s super-diffusive regime follows.

Richardson’s approach is exact if we assume that tracers disperse in a  $\delta$ -correlated in time velocity field. In such a case, the probability density function (PDF) of observing two tracers at separation  $r$  at time  $t$ ,  $P(r, t | r_0 t_0)$ , satisfies a Fokker-Planck diffusive equa-

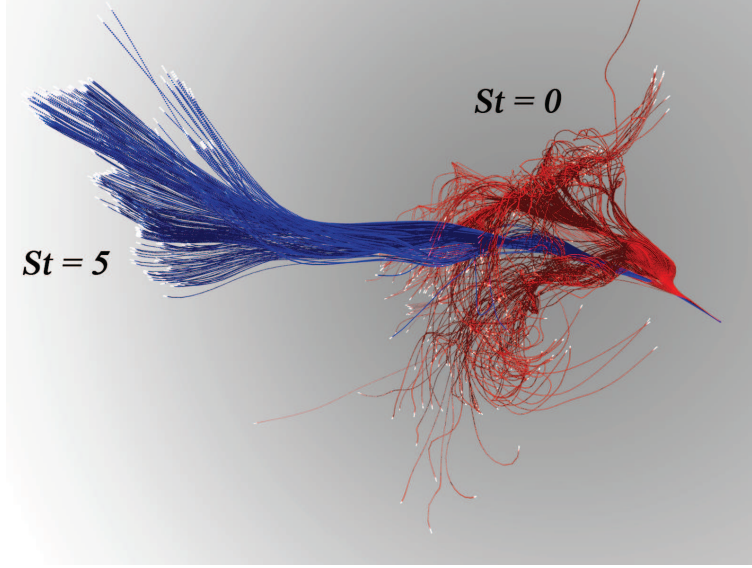


FIGURE 1. (color online). An ensemble of tracer particles with  $St = 0$  (red) and heavy particles with  $St = 5$  (blue), simultaneously emitted from a source of size  $\sim \eta$ . Trajectories are recorded from the emission time, up to the time  $t = 75\tau_\eta$  after the emission.

tion with a space dependent diffusivity coefficient,  $D(r)$  (Kraichnan 1966; Falkovich et al. 2001):

$$\frac{\partial P(r, t)}{\partial t} = \frac{1}{r^2} \frac{\partial}{\partial r} \left[ r^2 D(r) \frac{\partial P(r, t)}{\partial r} \right], \quad (1.5)$$

where  $D(r)$  is a function of the velocity correlation evaluated at the current separation, only.

The Richardson equation (1.5) with initial condition  $P(r, t_0) \propto \delta(r - r_0)$  can be solved, see e.g., Lundgren (1981); Bennett (2006), and the solution has an asymptotic, large time form (independent of the initial condition  $r_0$  and  $t_0$ ) of the kind:

$$P(r, t) = A \frac{r^2}{(k_0 \epsilon^{1/3} t)^{9/2}} \exp \left[ -\frac{9r^{2/3}}{4k_0 \epsilon^{1/3} t} \right], \quad (1.6)$$

where  $A$  is a normalization constant. The Richardson PDF is perfectly self-similar, so that all positive moments behave according to the dimensional law,  $\langle r^p \rangle \propto (\epsilon^{1/3} t)^{3p/2}$ .

There are many reasons for which the Richardson distribution cannot exactly describe the behaviour of tracer pairs in real flows. The most important ones are: (i) the nature of the temporal correlations in the fluid flow (Falkovich et al. 2001; Chaves et al. 2003); (ii) the non-Gaussian fluctuations of turbulent velocities (Frisch 1995); (iii) the small-scale effects induced by the dissipation sub-range, and (iv) the large-scale effects induced by the flow correlation length. These last two are of course connected to finite Reynolds-number effects.

It is worth noticing that formally any diffusion coefficient of the form  $D(r, t) \sim r^\alpha t^\beta$ , with  $3\alpha + 2\beta = 4$ , is compatible with the  $\sim t^3$  law, however different results would then be obtained for the functional form of  $P(r, t)$  (Monin & Yaglom 1975).

Since Richardson's seminal work, pair dispersion has been addressed in a large number of experimental and numerical studies, in the  $2d$  inverse energy cascade (Jullien et al. 1999; Boffetta & Celani 2000; Boffetta & Sokolov 2002a) and in the direct enstrophy cascade

(see e.g., Jullien (2003)), as well as in the 3d direct energy cascade (Biferale et al. 2005a; Ott & Mann 2000), in convective turbulent flows (Schumacher 2008; Ni & Xia 2013; Mazzitelli et al. 2014) and in synthetic flows (Fung & Vassilicos 1998; Malik & Vassilicos 1999; Thomson & Devenish 2005; Nicolleau & Nowakowski 2011). In Sawford et al. (2005), kinematic and direct numerical simulations have also been used to compare forward and backward relative dispersion in three dimensional turbulent flows. Comprehensive reviews on the topic can be found in Sawford (2001), Falkovich et al. (2001) and Salazar & Collins (2009).

Despite the huge amount of theoretical, numerical and experimental works devoted to this issue, it is fair to say that at the moment there is neither a clear consensus in favour of the Richardson's approach, nor a clear disproof. The main practical reason is due to the fact that the predictions -if correct-, are applicable to tracer pairs whose evolution has been for all times in the inertial range of scales:

$$\eta \ll r(t') \ll L \quad \forall t' \in [t_0, t], \quad (1.7)$$

where  $\eta$  is the viscous scale of the turbulent flow. In other words, we should record tracer dispersion at space and time scales *unaffected* by viscous or integral scale effects. This is of course a strong requirement which is particularly difficult to match in any experimental or numerical test because of the natural limitations in the accessible Reynolds number  $Re_\lambda$ , i.e., in the scale separation range  $Re_\lambda \propto (L/\eta)^{2/3}$ . Moreover the viscous scale itself  $\eta$  and the stretching rate at this scale are strongly fluctuating quantities in turbulent flows (Frisch 1995; Schumacher 2007; Yakhot 2006; Biferale 2008), causing further difficulties when pair statistics must be limited to a pure inertial range behaviour. It is worth noticing that a possible way out is to resort to exit-time statistics (Artale et al. 1997; Boffetta & Sokolov 2002a; Biferale et al. 2005a), which will be discussed in Section 4.

To avoid viscous effects on the pair dispersion statistics, it is also common to study pairs whose initial separation is well inside the inertial range,  $r(t_0) \gg \eta$ , paying the price to be dominated for long times by the initial condition and therefore mostly accessing the Batchelor regime (Bourgoin et al. 2006; Bitane et al. 2012a). Alternatively, numerical simulations of particles evolving in stochastically generated velocity fields are a useful tool to describe (possibly non Gaussian and non self-similar) inertial range pair dispersion (Kurbanmuradov 1997; Boffetta et al. 1999; Malik & Vassilicos 1999; Thomson & Devenish 2005). Note however that kinematic simulations might lead to a mean-square separation of the particle pairs with a power law different from the Richardson's law (Thomson & Devenish 2005).

For the reasons (i)-(ii) listed above, it is well possible that even in a infinite Reynolds number limit, the Richardson's prediction may turn out to be wrong. Effects of time correlations have been discussed by many authors (Klafter et al. 1987; Sokolov 1999; Bitane et al. 2012a; Scatamacchia et al. 2012; Eyink 2013), in connection to the problem of the formally admissible *infinite propagation speed* present in any diffusive approach *à la* Fokker-Planck (Masoliver & Weiss 1996; Kanatani et al. 2009; Ilyin et al. 2013), and also in relation to the possible non-Markovian nature of the Lagrangian position and velocity process (Thalaberd et al. 2014).

Summarising, it is extremely important to clarify with high accuracy if the deviations from Richardson's theory observed in laboratory experiments and numerical simulations, at finite Reynolds numbers, are due to sub-leading effects associated to the lack of scale-separation or not. In the latter case, it means that they would survive even in the  $Re \rightarrow \infty$  limit. This is the aim of the research presented in this paper.

We use Direct Numerical Simulations of isotropic and homogeneous three dimensional turbulence at  $Re_\lambda \sim 300$ , seeded with an unprecedented number of particles (emitted

from localised sources in different locations inside the flow), in order to increase the total number of pairs starting with an initially small separation and to minimise local anisotropy and non-homogeneity.

We present results for both tracers and point-like heavy particles, without feedback on the flow as in the original problem attacked by Richardson. When particles have inertia, new scenarios arise (Fouxon & Horvai 2008; Bec et al. 2010a), because of the non homogeneous spatial distribution (Bec et al. 2006a) and the very intermittent nature of relative velocity increments characterised by the presence of quasi-singularities (Falkovich et al. 2002; Wilkinson & Mehlig 2005; Bec et al. 2010b, 2011; Pan & Padoan 2010; Salazar & Collins 2012).

Not surprisingly, and in the absence of a theory, empirical observations are in this case even less stringent, also because of the need to specify the initial distributions of both particle positions and velocities. Two types of experiments can be done with inertial particles. The first consists of studying relative dispersion as a function of the distribution of initial separations only. In practice, inertial particles are allowed to reach their stationary spatial and velocity distributions inside a bounded volume (stationary distribution on a fractal dynamical attractor in phase-space), after which their dispersion properties are measured, conditioning on the initial distance (Bec et al. 2010a). The second consists in directly injecting inertial particles in the flow, with prescribed initial velocity and separation distributions. The first protocol is more relevant to study relative dispersion properties in connection with spatial clustering, particularly effective at small Stokes numbers (e.g., the spatial preferential concentration and trapping in coherent structures in the flow), and in connection with caustics, strongly modifying the relative velocities at large Stokes numbers (Abrahamson 1975; Bec et al. 2010a,b; Pan & Padoan 2010). The second protocol is more relevant in geophysical and industrial applications, where transient behaviours are crucial as in the case of volcanic eruptions, leakages of contaminants, or pollutant emissions.

In this paper, we are interested in the latter case, for which we designed the simplest procedure of having inertial particles emitted in the same positions and with the same velocities of the tracers (see Figure 1). This choice turns out to be optimal to better understand the statistics of tracers also, as it will become clearer in the sequel.

The main results of the paper can be briefly anticipated. First, we quantify the importance of viscous-scale fluctuations for tracer separations, showing that they easily affect the separation evolution for time scales much larger than what predicted by the dimensional Batchelor time,  $t_B(r_0)$ . This effect is so huge that, in current experiments, it spoils any possibility to assess tracer scaling properties in the *expected* inertial range of time scales. To overcome this problem, we suggest that heavy pairs can be used as dispersing particles that are able to dynamically filter out viscous-time fluctuations. By measuring pair dispersion of heavy pairs at different degree of inertia, we are able to observe a much clearer convergence towards an inertial-range regime for the relative separation. We interpret this result as an indication of the existence of infinite Reynolds-number corrections to the Richardson's prediction, as expected on the basis of a Eulerian-Lagrangian multifractal approach (Borgas 1993; Boffetta et al. 1999; Biferale et al. 2004), yet never observed in real data. The multifractal approach (MF) is also used to determine a set of specific correlation moments involving powers of the pair separation distance and relative velocity of tracer pairs, which are expected to be statistically invariant along Lagrangian trajectories in the inertial range (Falkovich et al. 2001; Falkovich & Frishman 2013).

The paper is organised as follows. In section 2, we present the details of our numerical study. In section 3, we introduce the relative dispersion statistics for both tracers and heavy particles. In sub-section 3.1, we discuss the effects due to finite Reynolds numbers

---

$Re_\lambda$	$N^3$	$\eta$	$\Delta x$	$\epsilon$	$\nu$	$\tau_\eta$	$T_E$	$u_{rms}$	$N_p$	$N_{sou}$	$N_{tot}$	$T_{traj}$
280	$1024^3$	0.005	0.006	0.81	0.00088	0.033	67	1.7	$2 \times 10^3$	256	$4 \times 10^{11}$	160

---

TABLE 1. Parameters of the numerical simulations: Taylor-scale based Reynolds number  $Re_\lambda$ , grid resolution  $N^3$ , Kolmogorov length scale  $\eta$  in simulation units (SU), grid spacing  $\Delta x$  (SU), mean energy dissipation  $\epsilon$  (SU), kinematic viscosity  $\nu$  (SU), Kolmogorov time-scale  $\tau_\eta$  (SU), large-scale eddy turnover time  $T_E$  (in units of  $\tau_\eta$ ), root-mean-square velocity  $u_{rms}$  (SU),  $N_p$  number of trajectories of inertial particles emitted for each Stokes number  $St$  from each local source and for each puff,  $N_{sou}$  number of sources in the flow,  $N_{tot}$  total number of particle pairs emitted in all simulations per Stokes number (10 runs with 256 local sources, each emitting 80 puffs),  $T_{traj}$  maximal temporal length of particle trajectories (in units of  $\tau_\eta$ ).

---

and those induced by the fluctuations of the viscous scale. In sub-section 3.2, we present the numerical data for the probability density functions. In connection with the issue of intermittent corrections, in sub-section 3.3, we briefly review the multifractal prediction for the pair dispersion of tracers developed by (Boffetta et al. 1999), and we test it against our data. In section 4, we discuss the results concerning the exit-time statistics, probing pairs which separate very slowly.

## 2. Numerical details

The fluid is described by the Navier-Stokes equations for the velocity field  $\mathbf{u}(\mathbf{x}, t)$

$$\partial_t \mathbf{u} + \mathbf{u} \cdot \nabla \mathbf{u} = -\nabla p + \nu \nabla^2 \mathbf{u} + \mathbf{f}, \quad \nabla \cdot \mathbf{u} = 0. \quad (2.1)$$

The statistically homogeneous and isotropic external forcing  $\mathbf{f}$  injects energy in the first low-wavenumber shells, by keeping constant in time their spectral content (Chen et al. 1993). The kinematic viscosity  $\nu$  is chosen such that the Kolmogorov length scale is  $\eta \simeq \delta x$ , where  $\delta x$  is the grid spacing, so that a good resolution of the small-scale velocity dynamics is obtained. The numerical domain is cubic, with periodic boundary conditions in the three space directions; a fully dealiased pseudo-spectral algorithm with second-order Adam-Bashforth time-stepping is used. We performed a series of Direct Numerical Simulations with resolution of  $1024^3$  grid points and Reynolds number at the Taylor scale  $Re_\lambda \simeq 300$ . The flow is seeded with bunches of tracers and heavy particles, emitted in different fluid locations to reduce the large scale correlations, and local inhomogeneous/anisotropic effects. Each bunch is emitted within a small region of space, of Kolmogorov scale size, in puffs of  $2 \times 10^3$  particles each, for tracers and heavy particles. In a single run, there are 256 of such point sources, releasing about 80 puffs with a frequency comparable with the inverse of the Kolmogorov time. We collected statistics over 10 different runs. As a result, we follow a total amount of  $4 \times 10^{11}$  pairs.

The heavy particles are assumed to be of size much smaller than the Kolmogorov scale of the flow and with a negligible Reynolds number relative to the particle size. In this limit, their equations of motion take the simple form:

$$\dot{\mathbf{X}}(t) = \mathbf{V}(t), \quad \dot{\mathbf{V}}(t) = -\frac{1}{\tau_s} [\mathbf{V}(t) - \mathbf{u}(\mathbf{X}, t)], \quad (2.2)$$

where the dots denote time derivatives. The particle position and velocity vectors are  $\mathbf{X}(t)$  and  $\mathbf{V}(t)$ , respectively;  $\mathbf{u}(\mathbf{X}, t)$  is the Eulerian fluid velocity evaluated at the particle position. The particle response time is  $\tau_s$ . The flow Kolmogorov time scale, appearing in the definition of the Stokes number,  $St = \tau_s / \tau_\eta$ , is  $\tau_\eta = (\nu / \epsilon)^{1/2}$ . Particle-particle

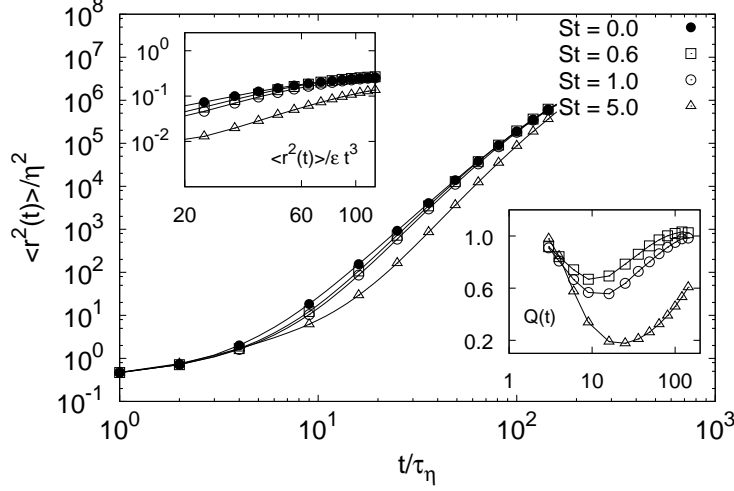


FIGURE 2. (Main body) Log-log plot of the mean-square separation versus time for particle pairs at changing inertia. (Upper inset) Log-log plot of the same curves, compensated with the Richardson’s inertial range behavior. (Lower inset) The ratio  $Q(t)$ , in log-lin scale, of the mean-square separation of heavy particle pairs, normalised with the curve for tracer pairs.

interactions and the feedback of the particles onto the flow are here neglected. In this work, we show results for the following set of Stokes numbers:  $St = 0.0, 0.6, 1.0$  and  $5.0$ . Additional details of the runs can be found in Table 1.

### 3. Relative separation statistics

In Figure 1, we compare the time evolution up to a time of the order of the large scale eddy turn over time,  $T_E$ , of a bunch of tracers and a bunch of heavy particles with  $St = 5$ , both emitted in a region of strong shear.

At a time lag roughly equal to  $t = 10\tau_\eta$  after the emission, it can be observed an abrupt transition in the particle dispersion of tracers (red in the online version), occurring when most of the pairs reaches a relative distance of the order of  $10\eta$ . Later on, we again notice the presence of many pairs with mutual separations much larger than the mean one. The trajectories of the heavy particles (blue in the online version) show a different evolution. After the emission, they tend to remain at a mutual distance of the order of  $\eta$  for a very long time, thus dispersing much less. Because they respond to fluid fluctuations with a time lag of the order of their Stokes time, they tend to keep their initial velocity unchanged before relaxing onto the underlying fluid velocities. As a result, inertial particles behave as if their Batchelor time was much longer than that of tracers (in our DNS the latter is small,  $t_B(r_0, St = 0) \sim \tau_\eta$ , because the source is strongly localised). Our main observation here is that the larger the Stokes number, the longer is the filtering time that heavy particles apply to the local stretching properties of the carrying fluid: since inertia is moderate in the present experiment, this fact will allow us to have a very effective method to reduce effects from viscous scale fluctuations in the particles’ statistics and to better disentangle inertial range properties in the pair dispersion evolution.

This is more quantitatively understood in Figure 2, where the second order moment of the relative separation for tracers,  $St = 0$ , and heavy particles,  $St = 5$ , are plotted.

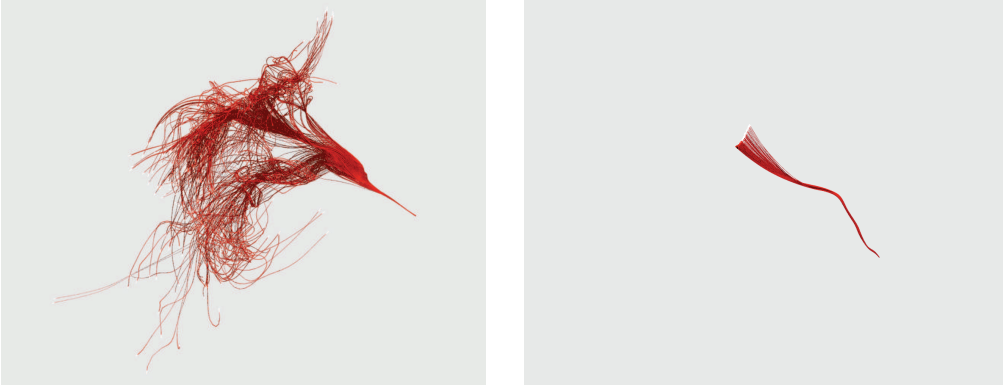


FIGURE 3. (color online) Left panel: The same ensemble of tracers reported in Figure 1. Right panel: Simultaneous realisation of a tracer bunch, emitted from a different source, showing a much smaller dispersion. Both emissions are recorded up to the time  $t = 75\tau_\eta$ .

Heavy particles tend to separate less since they are unaffected by turbulent fluctuations up to time and spatial scales large enough for their inertia to become sub-dominant with respect to the underlying turbulent fluctuations. On a dimensional ground, such a scale can be easily estimated to be of the order of  $r^*(St) \sim \eta St^{3/2}$  when  $St > 1$  (Bec et al. 2010a). Let us notice that in this respect the choice of the initially prescribed velocity distribution plays a key role, since inertial particles are emitted with a velocity equal to that of the underlying fluid. The quantity which is better suited to quantify this observation is the ratio between relative separations:

$$Q(t) = \frac{\langle r^2(t) \rangle_{St}}{\langle r^2(t) \rangle_0}.$$

In the present experiment we observe  $Q(t) < 1$  at any scale and time, as shown in the lower inset of Figure 2. By prescribing an initial distribution equal to the stationary PDF of heavy particle velocity increments, the trend would have been the opposite, with inertial particles at short times separating much faster than tracers, i.e.  $Q(t) > 1$  up to a separation  $r \simeq r^*(St)$  (Bec et al. 2010b). In the main body of Figure 2, we notice that for both tracers and heavy particles, and for time lags large enough, the separation curves tend toward a  $t^3$  Richardson-like behaviour, but without showing any clear scaling, as also measured by the compensated plot in the upper inset of Figure 2.

### 3.1. Viscous effects

To better appreciate the importance of viscous effects on pair dispersion, we show in Figure 3, the time evolution of two different bunches of tracers emitted in different positions in the flow. The initial size of the puffs is of the order of the viscous scale. The bunch on the left is emitted in a region where the stretching rate has a typical value of the order of its root mean square,  $\sim (\epsilon/\nu)^{-1/2}$ , while the bunch on the right is emitted in a region where the local stretching rate is unusually small. As a result this second bunch separates with a much longer delay with respect to the average behaviour.

In Figure 4, the mean squared separations measured for pairs belonging to each of these two bunches are compared with the pair separation averaged over the full statistics. The bunch emitted in a region where the stretching rate assumes the typical value exits the viscous region in a time lag of the order of  $\tau_\eta$ , and soon approaches the inertial range behaviour compatible with  $\sim t^3$ . Pairs belonging to the other bunch keep a small separation  $\langle r^2 \rangle^{1/2} \simeq \eta$  for a time lag up to  $\sim 50\tau_\eta$ , a time comparable to the integral



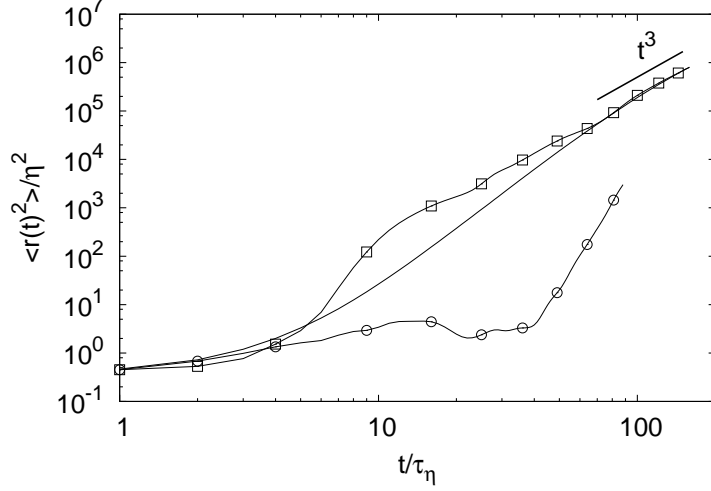


FIGURE 4. The mean-square separation behaviour for the two tracer emissions reported in Figure 3. Data from the left panel are represented by (□); while data from the right panel are represented by (○). The continuous curve is the mean square separation averaged over the whole statistical database.

time-scale  $T_E$ , and never recover the  $t^3$  scaling behaviour along the whole duration of our simulation. The examples shown in Figure 4 are meant to represent the huge variations that affect pair separation statistics for time lags of the order of  $\tau_\eta$ . These variations are the hardest obstacle to assess pure *inertial* range properties in any experimental or numerical set-up, in addition to the challenge of following particle trajectories for a time lag long enough – and in a volume large enough.

Our idea here is to use heavy particles as *smart* passive, but dynamical, objects to filter out such huge viscous effects, without affecting the long-time and large-scale physics. Indeed, heavy particles are less affected by fluctuations of the local viscous scale, since they respond to the fluid with their Stokes time (see Figure 1). Moreover, heavy pairs experience a less fluctuating local stretching rate, as also measured by the distribution of the finite-time Lyapunov exponents as a function of the Stokes number (Bec et al. 2006b). Finally, we recall that because of the injection choice here adopted, caustics in the heavy particles velocity distribution manifest themselves only at a later stage. As for the heavy pairs dispersion, the different degrees of fluctuations are better quantified in Figure 5, where we show the ratio of the third and fourth order moments of the separation distribution along the particle trajectories, normalised to the second order one

$$F_3(t) = \frac{\langle r^3(t) \rangle}{\langle r^2(t) \rangle^{3/2}}; \quad F_4(t) = \frac{\langle r^4(t) \rangle}{\langle r^2(t) \rangle^2}. \quad (3.1)$$

For convenience, we refer to  $F_3(t)$  and  $F_4(t)$  as generalised skewness and flatness, respectively. At the transition between the viscous and the inertial range of scales, i.e., for  $t \simeq 10\tau_\eta$ , tracers and small Stokes particles possess a generalised flatness  $F_4(t) \sim 100$ . This is the signature of an extremely intermittent distribution (for a  $\chi$ -squared distribution with three degrees of freedom, we would have  $F_4 = 3.1$ , while for the Richardson distribution  $F_4 = 7.81$ ). Moreover, it is evident that the bump displayed by the generalised flatness around  $10\tau_\eta$  is influenced by the behaviour at shorter times and influences the behaviour at much larger times. In other words, it is the quantitative counterpart of

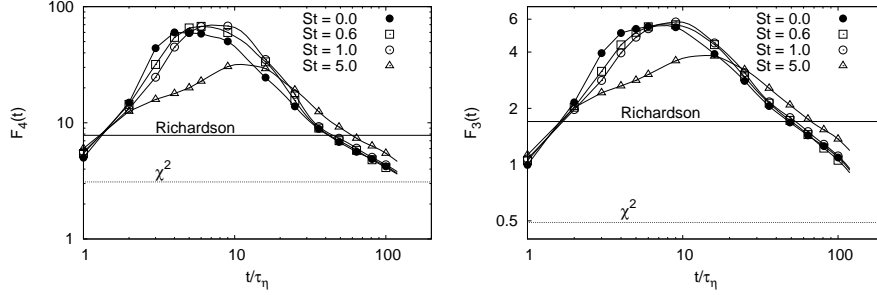


FIGURE 5. Generalised flatness (left) and skewness (right) of the relative dispersion probability density function, for pairs of different inertia. Horizontal lines refer to the Richardson expectations for these observable, which are 7.81 and 1.7, respectively; also plotted are the expected values for a  $\chi$ -squared distribution with three degrees of freedom, which are 3.1 for the flatness and 0.49 for the skewness.

the big variations shown in the two examples in Figure 4.

The filtering effect of the particle Stokes time is the reason for which heavy pairs initially possess a smaller flatness. This is particularly evident for the  $St = 5$  case, which exhibits a smoother transition toward a scaling behaviour for  $t > 10 - 20\tau_\eta$ , supporting the idea the inertia helps to remove viscous fluctuations from the physics of the inertial range. At time lags  $20\tau_\eta$ , the generalised coefficients  $F_3(t)$  and  $F_4(t)$  for heavy particles with  $St = 5$  are larger than those of the tracer pairs. This is probably the result of the relaxation onto the tracer power-law behaviour, which happens only at a later stage. Finally, it is clear from Figure 5 that the data set at the moderate inertia of  $St = 5$  is less affected by the strong viscous bump at  $t \sim 10\tau_\eta$  and that therefore promises to be the best candidate to test inertial range statistical properties.

### 3.2. Probability density functions

The probability density functions  $P(r, t)$  are plotted in Figure 6, for different values of inertia  $St = 0, 0.6, 1$  and  $5$ , and at different time lags after the emission from the source. In order to highlight the dynamics of those particles filling the left tail (i.e. separating less than the average), for Figure 6 we have selected pairs with initial separation  $r(t_0) \in [0.2 : 2]\eta$  (Bitane et al. 2012b). Consider first the behaviour at large separations. One clearly sees the effect anticipated earlier. Heavy particles tends to separate less. The effect becomes less and less visible with time, because inertia is forgotten on a time scale roughly proportional to the Stokes time. Pairs with  $St = 5$ , however, accumulate a delay in separation that is never recovered, even at large times  $t \sim 50\tau_\eta$ .

For the left tails, associated to pairs that do not separate, the trend as a function of Stokes is the opposite. We recall that from classical arguments (Falkovich et al. 2001), we expect that the fraction of tracer pairs at a distance  $r$  would behave as a power law  $r^{d-1}$ , where  $d = 3$  is the space dimension, see eq. (1.6). Similarly, for heavy pairs, we expect to observe the scaling  $P(r) \propto r^{D_2-1}$ , where  $D_2(St) \neq d$  measures the spatial correlation dimension. At short time lags,  $t \simeq 5\tau_\eta$ , the effect of inertia quickly appears and we measure a higher probability to observe pairs at very small separations: this happens because heavy pairs are less affected than tracers by intermittent events of anomalously slow separations, and hence rapidly populate the left tail of the distribution. As time goes on,  $t \simeq 20\tau_\eta$ , we observe that pairs with moderate inertia, namely  $St = 0.6$  and  $St = 1$ , clearly show the tendency to clusterise on a fractal set (Balkovsky et al. 2001; Boffetta et al. 2004; Bec 2005; Chun et al. 2005; Bec et al. 2006a) characterised by the spatial correlation

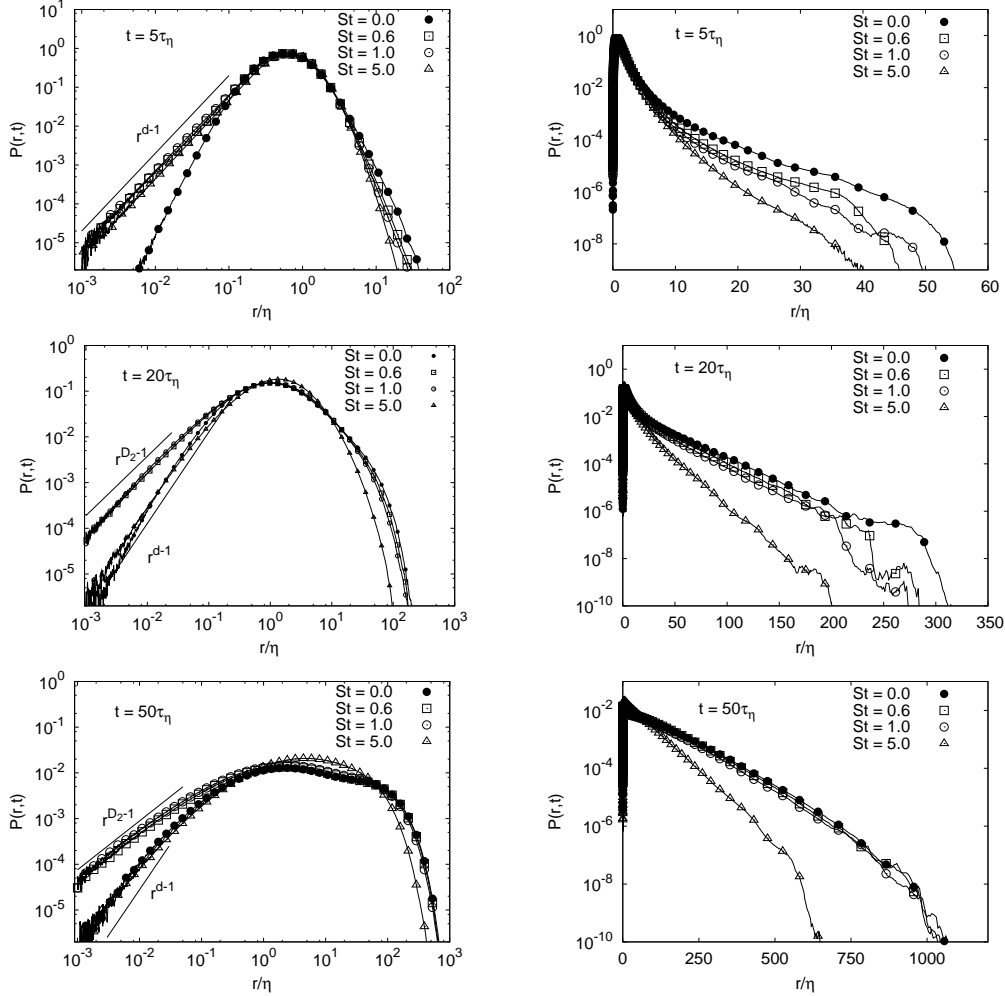


FIGURE 6. (Left panels) Log-log plot of separation PDFs  $P(r, t)$  for pairs with different inertia  $St = 0.0, 0.6, 1.0, 5.0$  highlighting the left tails behaviour. Plots refer to times  $5\tau_\eta$ ,  $20\tau_\eta$  and  $50\tau_\eta$  after the emission. The power-law scaling  $r^{d-1}$ , with  $d = 3$ , is plotted. The power-law scaling  $r^{D_2-1}$  is also reported: note that for  $St = 0.6$  the correlation dimension  $D_2(St)$  is  $2.27 \pm 0.03$ , while for  $St = 1.0$  it is  $D_2(St) = 2.31 \pm 0.03$  (Bec et al. 2011). The two power laws  $r^{D_2-1}$  for  $St = 0.6$  and  $St = 1.0$  are indistinguishable in the scale of the plot, hence we reported the slope for  $St = 1.0$  only. (Right panels): Lin-log plot of the same separation PDFs, at the same time lags. For these PDFs pairs are selected with initial separation  $r_0 \in [0.2 : 2]\eta$ .

dimension  $D_2(St) < d$  (Bec et al. 2006a, 2007), where  $d$  is the spatial dimension of the flow. Differently, we clearly observe that the left tail of the tracer PDF superposes well with that of the largest Stokes,  $St = 5$ : this is because the correlation dimension for this high Stokes number is  $D_2(St = 5) \simeq d$ . At a later time lag,  $t \simeq 50\tau_\eta$ , it is very hard to detect a power-law scaling in the left tail, even with the large database of the present experiment: by this time lag, most of the pairs have reached larger separations. Since pair dispersion takes place at finite Reynolds numbers, it is clear that asymptotic power-law behaviours, see eq. (1.6), can be observed in a limited range of space and time scales, only. To summarise, the observed power-law scalings at small separations reproduce the

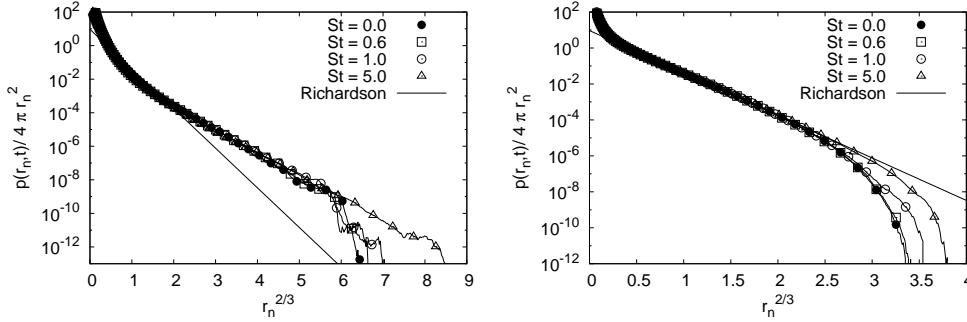


FIGURE 7. Lin-log plot of the pair separation PDFs in rescaled units,  $r_n = r / \langle r^2(t) \rangle^{1/2}$ , at time lags  $20\tau_\eta$  (left panel) and  $80\tau_\eta$  (right panel), for different Stokes numbers.

classical expectations for tracers and heavy pairs reported in Falkovich et al. (2001), and based on the Richardson's model. To detect intermittency effects, that we expect to be present due to tracer pairs that separate much less than the average, different observables are needed. This will be the object of the exit-time analysis in the last section.

Things become more interesting when the pair separation distribution are plotted in dimensionless units. In Figure 7, we show the PDFs measured over the whole statistical database, as a function of the pair distance and also in terms of the normalised relative separation,

$$r_n = \frac{r}{\langle r^2(t) \rangle_{St}^{1/2}}.$$

It is important to notice that the differences as a function of the Stokes number previously observed are fully reabsorbed once dimensionless quantities are used. This supports a strong universality for large separations as a function of  $St$ , at least up to the values here studied. Should the PDF data follow the Richardson's prediction, we would see a perfect rescaling on a stretched exponential curve, for all times and all separations. It is evident that this is not the case. Moreover, we stress that the most important departures from the Richardson's prediction develop on the far right tails, i.e. for intense fluctuations due to pairs that separate much more than the average. This fact was already observed using the same dataset by Scatamacchia et al. (2012). Previous numerical and experimental studies were limited to events with a probability larger than  $10^{-6}$  (see e.g., Ott & Mann (2000); Biferale et al. (2005a)), where departures from the Richardson's prediction could not be unambiguously detected.

It must be noticed that the renormalisation in terms of the separation  $r_n$  brings some extra difficulties in the interpretation of data. Indeed, since the mean squared separation,  $\langle r^2(t) \rangle_{St}^{1/2}$ , is increasing with time, at large times it might well happen that the far right tails of the PDFs are completely dominated by large-scale effects,  $r \sim L$ . The opposite happens for the events close to the peak, which can be affected by viscous contributions,  $r \sim \eta$ , for small times. In both cases, finite Reynolds-number effects come into play. As a result, these rescalings do not allow straightforward conclusions, neither to confirm neither to exclude the alleged departures from the distribution predicted by Richardson in the infinite Reynolds limit.

In Figure 8 we show the same data of Figure 7, but conditioning the relative separation to belong to the inertial range of scales,  $25\eta < r < 300\eta$ . A more coherent picture now emerges, since we note that (i) curves belonging to different time lags develop clearly non overlapping tails; (ii) for times large enough a universal, Stokes independent, regime

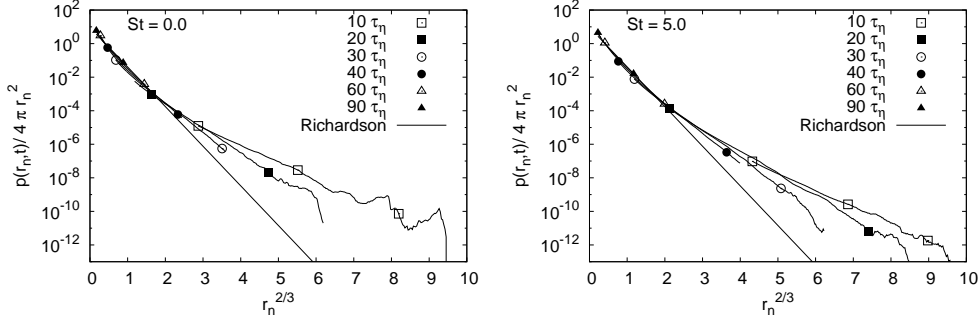


FIGURE 8. Lin-log plot of the rescaled pair separation PDFs at times lags  $t = (10, 20, 30, 40, 60, 90)\tau_\eta$ , selecting the pair distances to be in the range  $r \in [25, 300]\eta$ . Left panel is for tracers, while the right panel is for heavy pairs with  $St = 5$ . Symbols are drawn for a subset of points only for clarity.

seems to develop; (iii) the rapid fall-off of the left tails of the PDFs for extreme separations disappears. These observations suggest the possibility to identify inertial range statistical properties that show a Reynolds-independent departure from the Richardson's prediction and that can not be attributed to viscous or large-scale effects.

### 3.3. The Multifractal prediction for pair dispersion

The presence of inertial-range deviations from the pure self-similar behaviour of pair separation statistics predicted by the Richardson's approach should not be surprising, although never observed. In the  $3d$  direct energy cascade regime, anomalous scaling is measured both in the statistics of Eulerian longitudinal and transverse velocity increments (Frisch 1995; Sreenivasan & Antonia 1997; Biferale et al. 2008), and in the statistics of Lagrangian velocity increments along single particle trajectories (Mordant et al. 2001; Biferale et al. 2004; Xu et al. 2006; Arneodo et al. 2008; Biferale et al. 2011). A simple argument predicts the presence of intermittent corrections in the high-order moments of the relative particles separation,  $\langle r^p \rangle$  (Novikov 1989; Boffetta et al. 1999). The starting point is the exact relation for the moment of order  $p$  of the pair separation,

$$\frac{d}{dt} \langle r^p \rangle = p \langle r^{p-1} (\delta_r u) \rangle, \quad (3.2)$$

where  $\delta_r u$  is the velocity increment measured along the tracer pair trajectories, separated by a distance  $r$ . Here, for simplicity, we have neglected the tensorial structure and the time dependency of  $r$  and  $\delta_r u$  is understood. Let us suppose that the above correlation can be estimated with fully Eulerian quantities, then the multifractal approach Frisch (1995) could be employed to obtain:

$$\langle r^{p-1} (\delta_r u) \rangle \propto \int dh r^{3-D(h)} r^{p-1} r^h, \quad (3.3)$$

where  $P(h) \propto r^{3-D(h)}$  is the probability to observe an Eulerian velocity fluctuation at the scale  $r$  with a local scaling exponent  $h$ ,  $\delta_r u \sim r^h$ , as a function of the spectrum of fractal dimension,  $D(h)$ . In order to relate the above Eulerian estimate with the Lagrangian one in (3.2), one can adopt the dimensional *bridge* relation supposing that Lagrangian velocity fluctuations at separation  $r(t)$  are connected to Eulerian spatial fluctuations at scale  $r$  with  $t \sim r/\delta_r u \sim r^{1-h}$ . This amounts to say that one can use the same fractal dimensions  $D(h)$  for the Lagrangian and Eulerian velocity statistics. A quantitative support for this hypothesis has been made by a validation for one particle quantities against numerical

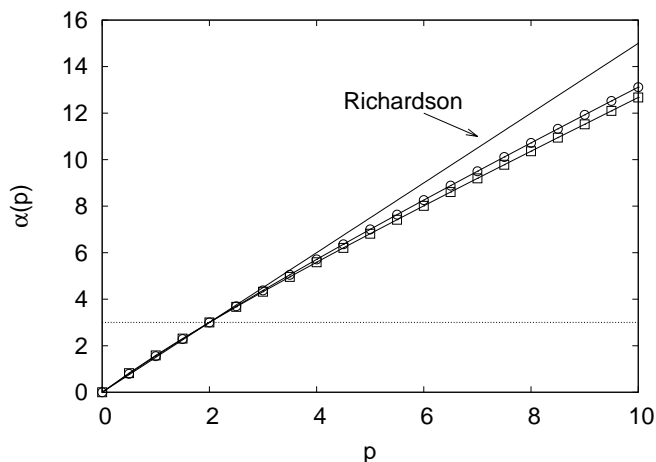


FIGURE 9. Multifractal exponents for pair separation statistics, derived from the scaling exponents of the Eulerian longitudinal structure functions,  $D_L(h)$  ( $\circ$ ), and from the scaling exponents of Eulerian transversal structure functions,  $D_T(h)$  ( $\square$ ). The continuous line is the dimensional Richardson scaling,  $\alpha(p) = 3p/2$ .

and experimental results in Arneodo et al. (2008). The same argument applied to two-particle quantities allows to rewrite (3.3) as a function of the time lag,  $t$ , along the particle separations,

$$\langle r^{p-1}(\delta_r u) \rangle \propto \int dh t^{\frac{2-D(h)+p+h}{1-h}}. \quad (3.4)$$

After time integration, a saddle point approximation can be used in the limit  $t \rightarrow 0$ , when the smallest exponent dominates the integral (Boffetta et al. 1999):

$$\langle r^p(t) \rangle \propto t^{\alpha(p)}, \quad \alpha(p) = \min_h \frac{(3 - D(h) + p)}{(1 - h)}. \quad (3.5)$$

This is the multifractal theory for tracer pair separation statistics in the presence of an Eulerian velocity field (Boffetta et al. 1999), whose multiscale statistics is described by the set of fractal dimension  $D(h)$ . To our knowledge, such a prediction has never been tested, either on experimental or on numerical data, except for the validation against stochastic velocity fields reported in Boffetta et al. (1999). Note that the multifractal spectrum is in general non-linear in the order  $p$ ; since by the 4/5-law, the exponent of the third order longitudinal Eulerian structure function must be unity, we must also have that  $\alpha(2) \equiv 3$  (Novikov 1989; Boffetta et al. 1999). In Figure 9, we compare the multifractal spectrum,  $\alpha(p)$ , obtained by using two possible forms for  $D(h)$  (extracted, respectively, from the longitudinal Eulerian structure functions,  $D_L(h)$ , and from the transverse ones,  $D_T(h)$ ) in statistically homogeneous and isotropic 3d turbulence. Such small uncertainty is to be considered as our prediction error on the shape of the function  $D(h)$ , which cannot be deduced by first principles. A more detailed discussion about this point can be found in Benzi et al. (2010).

To measure the scaling behaviours, we use the procedure known as Extended Self Similarity (ESS) Benzi et al. (1993), which amounts to study the relative scaling of moments with respect to a reference one, whose exponent is constrained by an exact relation. In Figure 10, the  $p$ -th order moment of particle separation is compensated with the second

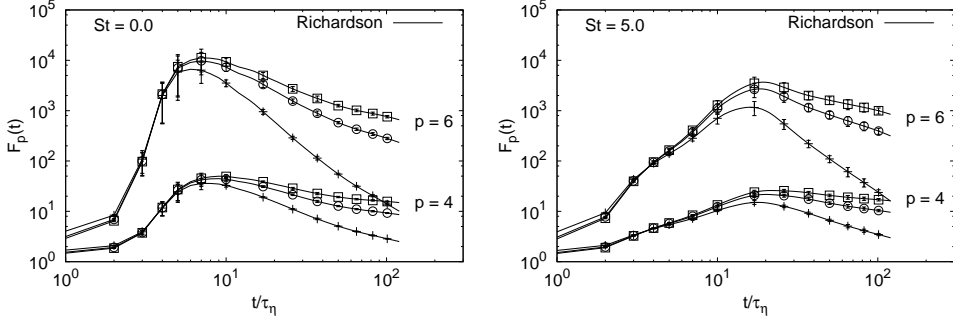


FIGURE 10. The ratio of pair separation moments of order  $p = 4$  and  $p = 6$  to the second order one, as a function of time. For each moment, the upper curve is obtained by compensating with the multifractal exponent,  $\alpha(p)$ , obtained from the Eulerian transverse structure functions, while the middle curve is obtained by compensating with the multifractal exponent from the Eulerian longitudinal structure functions (see previous figure and discussion in the text). The lower curve is obtained by compensating with the Richardson's dimensional scaling  $\alpha(p) = 3p/2$ . (Left) Moments of tracer separation; (right) moments of separation of heavy pairs with  $St = 5$ . The error bars are given by the root mean square of equation (3.6) computed on two equal sub-ensembles of the whole statistics.

order one:

$$F_p(t) = \frac{\langle r^p(t) \rangle}{\langle r^2(t) \rangle^{\frac{\alpha(p)}{3}}}, \quad (3.6)$$

both for tracer pairs and for heavy pairs at  $St = 5$ . In the inertial range where the prediction of equation (3.5) is expected to be valid, we should observe a plateau. It is evident that the multifractal prediction works better than the dimensional one, suggesting that the approach goes in the right direction. However, because the plateau is very narrow it is necessary to wait for data at higher Reynolds before making any firm conclusion. The claim is that the observed departure from the multifractal prediction in the tracers statistics is due to contamination induced by viscous effects, which we have seen to be very strong for the  $St = 0$  case. The situation becomes more interesting for heavy particles at  $St = 5$  for which viscous effects have a smaller impact. Here the multifractal scaling gives a larger plateau for the  $p = 4$  moment, and shows the beginning of a plateau for the  $p = 6$  moment. We thus have an indication of an inertial-range intermittent effect for particle pair separation statistics in homogeneous and isotropic 3d turbulence. This is the main result of this paper.

On the basis of the multifractal formalism, it is straightforward to conclude that there exist correlation functions that should be *statistically preserved* along pair trajectories, for scales well within the inertial range (Falkovich et al. 2001; Falkovich & Frishman 2013). Indeed, by again applying the saddle-point estimate to the inertial range scaling of the mixed separation-velocity moments, according to multifractal model we get that

$$C^{(p)}(t) = \langle r(t)^{-\zeta(p)} (\delta_{r(t)} u)^p \rangle \sim \text{const.} \quad (3.7)$$

if the scaling exponents of the particle separation compensates that of the Eulerian velocity moment:  $\zeta(p) \equiv \min_h(ph + 3 - D(h))$ . In Figure 11, we measure the mixed separation-velocity correlations of order  $p = 4$  and  $p = 6$  in ESS, that is with reference to the moment of order two. The scaling obtained by using the  $\zeta(p)$  exponents is the one that works better for inertial range time lags, i.e.  $t > 20\tau_\eta$ .

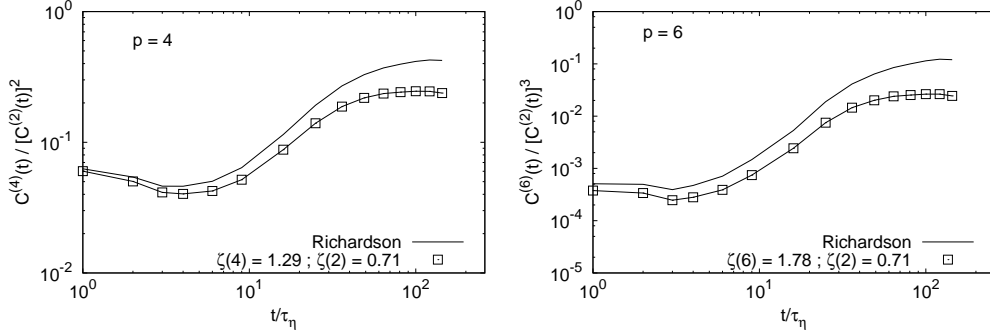


FIGURE 11. The ratio of mixed separation-velocity correlations  $C^{(p)}(t)$  of order  $p = 6$  and  $p = 4$ , with respect to a reference order,  $C^{(2)}(t)$ , vs time. The moments are compensated with the dimensional prediction of the theory of Richardson, and with the longitudinal intermittent scaling exponents.

#### 4. Exit-time statistics for tracers

Another interesting question concerns the statistical properties of *weak* separation events, i.e. the left tail of the probability density function. In order to assess the importance of these events, one cannot resort to negative moments of the separation statistics, because these are ill defined. An alternative approach which overcomes this difficulty is to use *inverse* statistics, see Jensen (1999), i.e., exit-times. Exit-times also allow for a clearer separation of scales as stressed by Boffetta & Sokolov (2002b). The idea consists in fixing a set of thresholds,  $r_n = \rho^n r_0$  with  $n = 1, 2, 3, \dots$  and  $\rho > 1$ , and in calculating the probability density function of the time  $T(r_n)$  needed for the pair separation to change from  $r_n$  to  $r_{n+1}$ . Formally this corresponds to calculating the first passage time. The advantage of this approach is that all pairs are sampled when they belong to eddies of similar size, between  $r_n$  and  $r_{n+1}$ . This limits the effect of pairs that at a given time lag, since they have separated very fast or very slow, might be at very different separation scales. In other words, in the exit-time statistics the *contamination* from viscous and large-scale cut-offs should be less important.

For particle pairs with initial condition  $P(r, t = 0) = \rho^2 \delta(r - r_n/\rho)/4\pi r_n^2$ , a perfectly reflecting boundary condition at  $r = 0$  and an absorbing boundary condition at  $r = r_n$ , the PDF of exit time,  $P(T)$ , is given by:

$$\mathcal{P}_{\rho, r_n}(T) = -\frac{d}{dt} \int_{|\mathbf{r}| < r_n} P(\mathbf{r}, t) d\mathbf{r}. \quad (4.1)$$

Using the Richardson's distribution of eq. (1.6) for  $P(\mathbf{r}, t)$ , we get

$$\mathcal{P}_{\rho, r_n}(T) = -4\pi k_0 \epsilon^{1/3} r_n^{10/3} \partial_r P|_{r=r_n}. \quad (4.2)$$

An asymptotic form of exit-time PDF behaves according to the following expression,

$$\mathcal{P}_{\rho, r_n}(T) \simeq \exp \left[ -\kappa \frac{\rho^{2/3} - 1}{\rho^{2/3}} \frac{T}{\langle T_\rho(r_n) \rangle} \right], \quad (4.3)$$

where  $\kappa \simeq 2.72$  is a dimensionless constant, for details see Biferale et al. (2005a), and  $\langle T_\rho(r_n) \rangle$  is the mean exit-time. Note that eq. (4.3) contains only dimensionless parameters and it is thus a universal result. We note that while positive moments  $\langle T_\rho^p(r_n) \rangle$  preferably sample pairs that separate slowly, negative moments,  $\langle [1/T_\rho(r_n)]^p \rangle$ , are dominated by pairs that separate fast, Boffetta & Sokolov (2002b). From eq. (4.3), a prediction can be



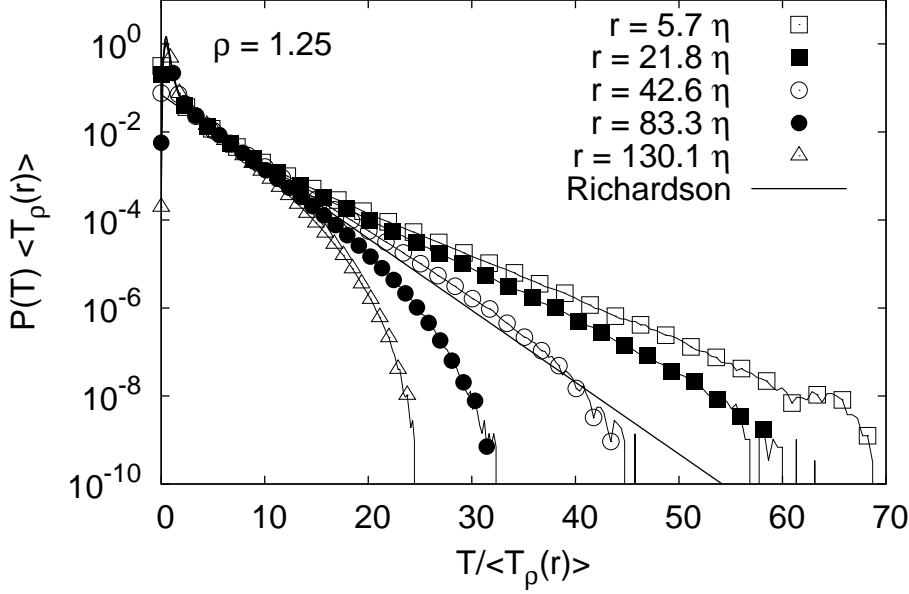


FIGURE 12. The exit-time PDFs for tracers pairs are shown, together with the Richardson's asymptotic form of the exit-time distribution. The growth factors for spatial thresholds is  $\rho = 1.25$ . The continuous straight line is the Richardson's prediction.

obtained for the mean exit-time (Boffetta & Sokolov 2002b),

$$\langle T_\rho(r) \rangle = \frac{1}{2 k_0 \epsilon^{1/3}} \frac{(\rho^{2/3} - 1)}{\rho^{2/3}} r^{2/3}, \quad (4.4)$$

from which it follows that according to the Richardson self-similar behaviour, we expect

$$\langle T_\rho^p(r) \rangle \propto r^{2p/3}. \quad (4.5)$$

In Figure 12, we plot the exit-time PDFs for the tracer pairs, calculated for  $\rho = 1.25$ . First, let us notice that the super-exponential decay observed for the large distance case is probably due to a systematic bias induced by the fact that we have a finite length in the trajectories and therefore very long exit times cannot be measured. Second, we observe that the curves do not overlap meaning that the PDFs are not self-similar. Concerning the statistical accuracy, this result is a clear improvement of the one reported in Biferale et al. (2005a): now deviations from the Richardson's prediction are evident because of the huge statistics achieved in the present numerical experiment. Even though the asymptotic distribution is still given by an exponential decay, as it should be expected from rare events following a Poissonian process, the whole PDF shape cannot be superposed using only the mean exit-time as a normalising factor.

Concerning the positive moments of the exit times, we use relative scaling properties to test a breaking of the self-similar properties. In Figure 13 we verify that we have the statistical convergence needed to measure moments of order  $\langle T_\rho^3(r) \rangle$  and  $\langle T_\rho^4(r) \rangle$ . In Figure 14, we show the ratio of  $T_\rho(r)$  moments of order  $p = 3, 4$  with respect to  $\langle T_\rho(r) \rangle^p$ , for  $\rho = 1.25$ . For separations within the inertial range  $r/\eta > O(10)$  the breaking of self-similarity is evident. It is difficult to conclude if these are true Reynolds independent corrections, and if they are affected by the finite length of the particle trajectories. More

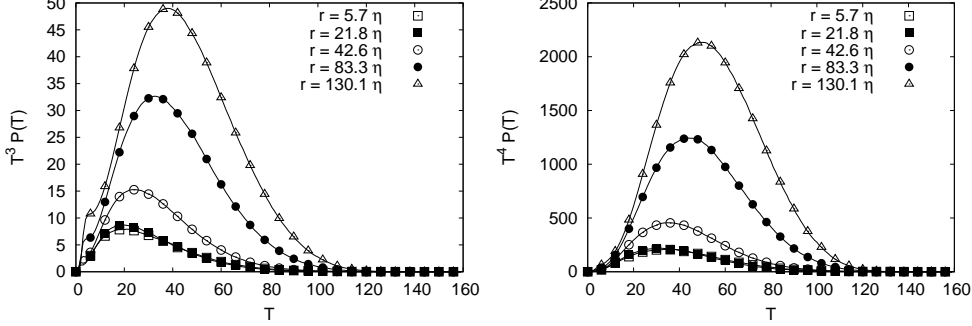


FIGURE 13. Products  $T_\rho^p P(T_\rho)$  with  $p = 3$  (left) and  $p = 4$  (right) for  $\rho = 1.25$ , testing the statistical convergence.

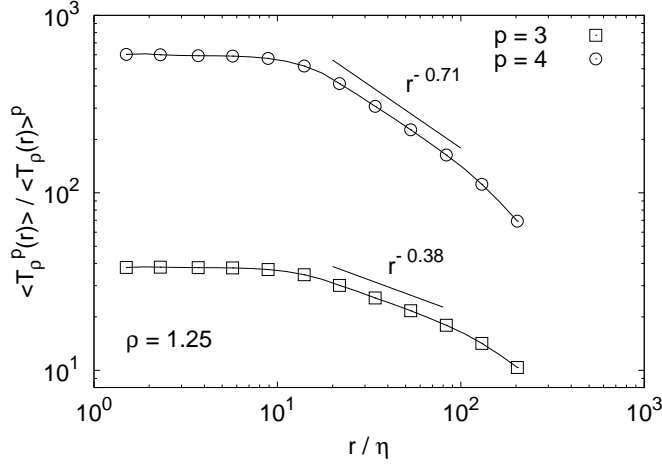


FIGURE 14. The ratio of positive exit-time moments of order  $p = 3$  and  $p = 4$  to  $\langle T_\rho(r) \rangle^p$ , as a function of thresholds for  $\rho = 1.25$ . For different values of  $\rho$  we observe the same behaviours.

data will be needed to get a more quantitative understanding of this effect. Furthermore, we recall that there is not a multifractal prediction for the behaviour of the positive exit-time moments of relative dispersion, since these would be associated to the negative moments of the Eulerian velocity increments (Jensen 1999).

## 5. Conclusions

In this work we have numerically studied the relative dispersion statistics of tracer and heavy particles emitted from point-like sources in a homogeneous and isotropic turbulent flow, at resolution  $1024^3$ . When particles are injected at separations of the order of the viscous scale, the fluctuations of the local stretching rate have a huge impact, influencing the mean square separation, up to time lags of the order of the integral time-scale. Such a dramatic effect has hindered the possibility of studying inertial range quantities in Lagrangian experiments or numerical simulations up to now. In this study, the large statistical database, the use of conditional statistics and the information obtained by comparing tracers and inertial particles evolution enabled us to highlight with a great precision, and for the first time, deviations in the pair separation distribution from the self-similar behaviour predicted by Richardson. Such deviations are manifest in the sta-

tistical behaviour of the right tail of the separation PDF, and are due to tracer pairs that separate much faster than the average. We use similar measurements for heavy particles at moderate inertia, which filter out fluctuations of the viscous scales, to give a higher confidence that the corrections observed for tracers are pure inertial range effect. Moreover, by conditioning the relative separation to belong to the inertial range of scales, a universal behaviour develops, which is Stokes independent and is clearly different from the Richardson's prediction. The behaviour of the conditioned PDFs support the idea that finite Reynolds-number effects, even if present, are sub-dominant. Furthermore, the numerical results indicate that tracer dispersion is intermittent, with deviations from a self-similar scaling visible already in the low order moments behaviour. The observed intermittent corrections to the Richardson's prediction are qualitatively consistent with a multifractal prediction for the scaling behaviour of relative separation moments of tracer pairs, although in a narrow scaling region. Numerical and experimental results at higher Reynolds number are requested to further support these findings. By measuring the exit-time statistics, we provide also an evidence of the non self-similar character of slow pair dispersion events. The statistics of the shapes of the puffs along the temporal evolution is also a crucial point that worths to be studied, involving more information about the multi-particle separation connected to geometry and shapes Chertkov et al. (1999); Biferale et al. (2005b); Xu et al. (2011)

We thank Jérémie Bec and Gregory Eyink for useful discussions. We acknowledge financial support from EU-COST Action MP0806 "Particles in Turbulence". This work is part of the research program of the Foundation for Fundamental Research on Matter (FOM), which is part of the Netherlands Organisation for Scientific Research (NWO). Numerical simulations were performed within the HPC Iskra Class A projects "Point" and "Flag" at CINECA (Italy). L.B. acknowledge partial funding from the European Research Council under the European Community's Seventh Framework Programme, ERC Grant Agreement N. 339032.

## REFERENCES

- ABRAHAMSON, J. 1975 Collision rates of small particles in a vigorously turbulent fluid. *Chem. Engng Sci.* **30**, 1371–1379.
- ARNEODO, A., ET AL. 2008 Universal Intermittent Properties of Particle Trajectories in Highly Turbulent Flows. *Phys. Rev. Lett.* **100**, 254504.
- ARTALE, V., BOFFETTA, G., CELANI, A., CENCINI, M. AND VULPIANI, A. 1997 Dispersion of passive tracers in closed basins: Beyond the diffusion coefficient. *Phys. Fluids* **9**, 3162–3171.
- BALDYGA, J. & BOURNE, J. R. 1999 *Turbulent Mixing and Chemical Reactions*. Wiley.
- BALKOVSKY, E., FALKOVICH, G. & FOUXON, A. 2001 Intermittent distribution of inertial particles in turbulent flows. *Phys. Rev. Lett.* **86**, 2790–2793.
- BATCHELOR, G.K. 1950 The application of the similarity theory of turbulence to atmospheric diffusion. *Q. J. Roy. Meteor. Soc.* **76**, 133.
- BEC, J. 2005 Multifractal concentrations of inertial particles in smooth random flows. *J. Fluid Mech.* **528**, 255–277.
- BEC, J., BIFERALE, L., BOFFETTA, G., CELANI, A., CENCINI, M., LANOTTE, A. S., MUSACCHIO, S., & TOSCHI, F. 2006 Acceleration statistics of heavy particles in turbulent flows. *J. Fluid Mech.* **550**, 349–358.
- BEC, J., BIFERALE, L., BOFFETTA, G., CENCINI, M., MUSACCHIO, S., & TOSCHI, F. 2006 Lyapunov exponents of heavy particles in turbulence. *Phys. Fluids* **18**, 091702.
- BEC, J., BIFERALE, L., CENCINI, M., LANOTTE, A.S., MUSACCHIO, S., & TOSCHI, F. 2007 Heavy Particle Concentration in Turbulence at Dissipative and Inertial Scales. *Phys. Rev. Lett.* **98**, 084502.

- BEC, J., BIFERALE, L., LANOTTE, A. S., SCAGLIARINI, A., & TOSCHI, F. 2010 Turbulent pair dispersion of inertial particles. *J. Fluid Mech.* **645**, 497–528.
- BEC, J., BIFERALE, L., CENCINI, M., LANOTTE, A. S., & TOSCHI, F. 2010 Intermittency in the velocity distribution of heavy particles in turbulence. *J. Fluid Mech.* **646**, 527–536.
- BEC, J., BIFERALE, L., CENCINI, M., LANOTTE, A. S., & TOSCHI, F. 2011 Spatial and velocity statistics of inertial particles in turbulent flows. *J. Phys.: Conf. Series* **333**, 012003.
- BENNETT, A. F. 1984 Relative dispersion: local and nonlocal dynamics. *J. Atmos. Sci.* **41**(11) 1881–1886.
- BENNETT, A. 2006 *Lagrangian Fluid Dynamics*. Cambridge University Press, Cambridge Monographs on Mechanics.
- BENZI, R., CILIBERTO, S., TRIPICCIONE, R., BAUDET, C., MASSAIOLI, F., SUCCI, S. 1993 Extended self-similarity in turbulent flows. *Phys. Rev. E* **48** R29.
- BENZI, R., BIFERALE, L., FISHER, R., LAMB, D.Q. & TOSCHI, F. 2010 Inertial range Eulerian and Lagrangian statistics from numerical simulations of isotropic turbulence. *Journ. Fluid Mech.* **653**, 221.
- BENZI, R. 2011 in *A voyage through turbulence*. Ed. P. Davidson, Y. Kaneda, K. Moffatt, and K. Sreenivasan. Cambridge University Press.
- BIFERALE, L., BOFFETTA, G., CELANI, A., DEVENISH, B. J., LANOTTE, A., & TOSCHI, F. 2004 Multifractal Statistics of Lagrangian Velocity and Acceleration in Turbulence. *Phys. Rev. Lett.* **93**, 064502, 1–4.
- BIFERALE, L., BOFFETTA, G., CELANI, A., DEVENISH, B. J., LANOTTE, A., & TOSCHI, F. 2005 Lagrangian statistics of particle pairs in homogeneous isotropic turbulence. *Phys. Fluids* **17**, 115101.
- BIFERALE, L., BOFFETTA, G., CELANI, A., DEVENISH, B. J., LANOTTE, A., & TOSCHI, F. 2005 Multi-particle dispersion in fully developed turbulence. *Phys. Fluids* **17**, 111701.
- BIFERALE, L. 2008 A note on the fluctuation of dissipative scale in turbulence. *Phys. Fluids* **20**, 031703.
- BIFERALE, L., LANOTTE, A.S. & TOSCHI, F. 2008 Statistical behaviour of isotropic and anisotropic fluctuations in homogeneous turbulence *Phys. D* **237**, 1969–1975.
- BIFERALE, L., CALZAVARINI, E. & TOSCHI, F. 2011 Multi-time multi-scale correlation functions in hydrodynamic turbulence. *Phys. Fluids* **23**, 085107.
- BITANE, R., HOMANN, H., & BEC, J. 2012 Time scales of turbulent relative dispersion. *Phys. Rev. E* **86**, 045302(R).
- BITANE, R., HOMANN, H., & BEC, J. 2012 Geometry and violent events in turbulent pair dispersion. *J. Turbulence* **14**, 23–45.
- BOFFETTA, G., CELANI, A., CRISANTI, A., & VULPIANI, A. 1999 Pair dispersion in synthetic fully developed turbulence *Phys. Rev. E* **60**, 6734–6741.
- BOFFETTA, G., & CELANI, A. 2000 Pair dispersion in turbulence. *Phys. A* **280**, 1–9.
- BOFFETTA, G. & SOKOLOV, I.M. 2002 Statistics of two-particle dispersion in two-dimensional turbulence. *Phys. Fluids* **14**, 3224.
- BOFFETTA, G. & SOKOLOV, I.M. 2002 Relative dispersion in fully developed turbulence: The Richardson’s Law and Intermittency Corrections. *Phys. Rev. Lett.* **88**, 094501.
- BOFFETTA, G., DE LILLO, F. & GAMBA, A. 2004 Large scale inhomogeneity of inertial particles in turbulent flows. *Phys. Fluids* **16**, L20–L24.
- BOURGOIN, M., OUELLETTE, N. T., XU, H., BERG, J. & BODENSCHATZ, E. (2006) The Role of Pair Dispersion in Turbulent Flow. *Science* **311**, 835.
- BORGAS, M. S. 1993 The Multifractal Lagrangian Nature of Turbulence. *Phil. Trans. R. Soc. Lond. A* **342**, 379–411.
- BORGAS, M. S. & SAWFORD, B. L. 1994 A family of stochastic models for two-particle dispersion in isotropic homogeneous stationary turbulence. *J. Fluid Mech.* **279**, 69–99.
- BORGAS, M. S. & YEUNG, P. K. 2004 Relative dispersion in isotropic turbulence. Part 2. A new stochastic model with Reynolds-number dependence. *J. Fluid Mech.* **503**, 125–160.
- CHAVES, M., GAWĘDZKI, K., HORVAI, P., KUPIAINEN, A. & VERGASSOLA, M. 2003 Lagrangian Dispersion in Gaussian Self-Similar Velocity Ensembles *J. Stat. Phys.* **113** 643–692.
- CHEN, S., DOOLEN, G. D., KRAICHNAN, R. H. & SHE, Z.-S. 1993 On statistical correlations between velocity increments and locally averaged dissipation in homogeneous turbulence. *Phys. Fluids A* **5**, 458.

- CHERTKOV, M., PUMIR, A., & SHRAIMAN, B.I. 1999 Lagrangian tetrad dynamics and the phenomenology of turbulence. *Phys. Fluids* **11**, 2394.
- CHUN, J., KOCH, D. L., RANI, S., AHLUWALIA, A. & COLLINS, L. R. 2005 Clustering of aerosol particles in isotropic turbulence. *J. Fluid Mech.* **536**, 219–251.
- CSANADY, G.T. 1973 *Turbulent diffusion in the environment*. Ed. D. Reidel Publishing Company.
- DIMOTAKIS, P. E. 2005 Turbulent Mixing. *Annu. Rev. Fluid Mech.* **37** 329–56.
- EYINK, G. 2013 Diffusion approximation in turbulent two-particle dispersion. *Phys. Rev. E* **88** 041001(R).
- FALKOVICH, G., GAWĘDZKI, K. & VERGASSOLA, M. 2001 Particles and Fields in Fluid Turbulence. *Rev. Mod. Phys.* **73**, 913–75.
- FALKOVICH, G., FOUXON, A. & STEPANOV, G. 2002 Acceleration of rain initiation by cloud turbulence. *Nature* **419**, 151.
- FALKOVICH, G. & FRISHMAN, A. 2013 Single flow snapshot reveals the future and the past of pairs of particles in turbulence. *Phys. Rev. Lett.* **110** 214502.
- FOUXON, I. & HORVAI, P. 2008 Separation of Heavy Particles in Turbulence. *Phys. Rev. Lett.* **100**, 04061.
- FRISCH, U. 1995 *Turbulence. The legacy of A. N. Kolmogorov*. Cambridge University Press.
- FUNG, J. C. H., & VASSILICOS, J.C. 1998 Two-particle dispersion in turbulent-like flows. *Phys. Rev. E* **57**, 1677.
- JENSEN, M.-H. 1999 Multiscaling and Structure Functions in Turbulence: An Alternative Approach. *Phys. Rev. Lett.* **83**, 76.
- JULLIEN, M.-C., PARET, J., & TABELING, P. 1999 Richardson Pair Dispersion in Two-Dimensional Turbulence. *Phys. Rev. Lett.* **82** 2872.
- JULLIEN, M.-C. 2003 Dispersion of passive tracers in the direct enstrophy cascade: Experimental observations. *Phys. Fluids* **15** 2228–2237.
- KANATANI, K., OGASAWARA, T., & TOH, S. 2009 Telegraph-type versus diffusion-type models of turbulent relative dispersion. *J. Phys. Soc. Jap.* **78**, 024401.
- KLAFTER, J., BLUMEN, A., & SHLESINGER, M.F. 1987 Stochastic pathway to anomalous diffusion. *Phys. Rev. A* **35**, 3081–3085.
- KRAICHNAN, R. H. 1966 Dispersion of Particle Pairs in Homogeneous Turbulence. *Phys. Fluids* **9**, 1937–1943.
- KURBANMURADOV, O. A. 1997 Stochastic Lagrangian models for two-particle relative dispersion in high-Reynolds number turbulence. *Monte Carlo Meth. Applic.* **3**, 37–52.
- ILYIN, V., PROCACCIA, I., & ZAGORODNY, A. 2013 Fokker-Planck equation with memory: the crossover from ballistic to diffusive processes in many-particle systems and incompressible. *Cond. Matt. Phys.* **16**, 13004-1.
- LACASCE, J.H. 2010 Relative displacement probability distribution functions from balloons and drifters. *J. Mar. Res.* **68**, 433–457.
- LACORATA, G., MAZZINO, A., & RIZZA, U. 2008 3D Chaotic Model for Subgrid Turbulent Dispersion in Large Eddy Simulations. *J. Atmos. Sci.* **65**, 2389–2401.
- LEPRETI, F., CARBONE, V., ABRAMENKO, V. I., YURCHYSHYN, V., GOODE, P. R., CAPPARELLI, V., & VECCHIO, A. Turbulent pair dispersion photospheric bright points. *Astrophys. J. Lett.* **759**, L17.
- LUNDGREN, T.S. 1981 Turbulent pair dispersion and scalar diffusion. *J. Fluid Mech.* **111**, 27–57.
- MALIK, N. A. & VASSILICOS, J. C. 1999 A Lagrangian model for turbulent dispersion with turbulent-like flow structure: Comparison with direct numerical simulation for two-particle statistics. *Phys. Fluids* **11**, 1572.
- MASOLIVER, J. & WEISS, G.H. 1996 Finite-velocity diffusion. *Eur. J. Phys.* **17**, 190–196.
- MAZZITELLI, I. M., FORNARELLI, F., LANOTTE, A.S. & ORESTA, P. 2014 Pair and multi-particle dispersion in numerical simulations of convective boundary layer turbulence. *Phys. Fluids* **26**, 055110.
- MONIN, A. S. & YAGLOM, A. M. 1975 *Statistical Fluid Mechanics* Cambridge, Mass. (USA): MIT Press, c1971-1975.
- MORDANT, N., METZ, P., MICHEL, O. & PINTON, J.-F. 2001 Measurement of Lagrangian velocity in fully developed turbulence. *Phys. Rev. Lett.* **87**, 214501.

- NI, R. & , XIA, K.-Q. 2013 Experimental investigation of pair dispersion with small initial separation in convective turbulence. *Phys. Rev. E* **87**, 063006.
- NICOLLEAU, F. C. G. A. & NOWAKOWSKI, A. F. 2011 Presence of a Richardson regime in kinematic simulations. *Phys. Rev. E* **83**, 056317.
- NOVIKOV, E. A. 1989 Two-particle description of turbulence, Markov property and intermittency. *Phys. Fluids A* **1**(2), 326–330.
- OLLITRAUT, M., GABILLET, C. & COLIN DE VERDIÈRE, A. 2005 Open ocean regimes of relative dispersion. *J. Fluid Mech.* **533**, 381–407.
- OTT, S. & MANN, J. 2000 An experimental investigation of the relative diffusion of particle pairs in three-dimensional turbulent flow. *J. Fluid Mech.* **422**, 207–223.
- PAGNINI, G. 2008 Lagrangian stochastic models for turbulent relative dispersion based on particle pair rotation. *J. Fluid Mech.* **616**, 357–395.
- PAN, L., & PADOAN, P. 2010 Relative velocity of inertial particles in turbulent flows. *J. Fluid Mech.* **661** 73–107.
- POULAIN, P.M. & ZAMBIANCHI, E. 2007 Surface circulation in the central Mediterranean Sea as deduced from Lagrangian drifters in the 1990s *Cont. Shelf Res.*, **27**, 981–1001.
- RICHARDSON, L. F. 1926 Atmospheric diffusion shown on a distance-neighbour graph. *Proc. R. Soc. London, Ser A* **110**, 709.
- SALAZAR, J. P. L. C. & COLLINS, L. R. 2009 Two-Particle Dispersion in Isotropic Turbulent Flows. *Annu. Rev. Fluid Mech.* **41** 405–432.
- SALAZAR, J. P. L. C. & COLLINS, L. R. 2012 Inertial particle relative velocity statistics in homogeneous isotropic turbulence. *J. Fluid Mech.* **696** 45–66.
- SAWFORD, B. 2001 Turbulent Relative Dispersion. *Annu. Rev. Fluid Mech.* **33**, 289–317.
- SAWFORD, B.L., YEUNG, P.K. & BORGAS, M.S. 2005 Comparison of backwards and forwards relative dispersion in turbulence. *Phys. Fluids* **17**, 095109.
- SCATAMACCHIA, R., BIFERALE, L., & TOSCHI, F. 2012 Extreme Events in the Dispersions of Two Neighboring Particles Under the Influence of Fluid Turbulence. *Phys. Rev. Lett.* **109**, 144501.
- SCHUMACHER, J. 2007 Sub-Kolmogorov-scale fluctuations in fluid turbulence. *Europhys. Lett.* **80**, 54001.
- SCHUMACHER, J. 2008 Lagrangian Dispersion and Heat Transport in Convective Turbulence. *Phys. Rev. Lett.* **100**, 134502.
- SOKOLOV, I.M. 1999 Two-particle dispersion by correlated random velocity fields. *Phys. Rev. E* **60**, 5528.
- SREENIVASAN, K.R. & ANTONIA, R.A. 1997 The Phenomenology of small-scale turbulence. *Annu. Rev. Fluid Mech.* **29**, 435–472.
- THALABARD, S., KRSTULOVIC, G., & BEC, J. 2014 Turbulent pair dispersion as a continuous-time random walk. <http://arxiv.org/abs/1405.7315>.
- THOMSON, D. J. 1990 A stochastic model for the motion of particle pairs in isotropic high-Reynolds- number turbulence, and its application to the problem of concentration variance. *J. Fluid Mech.* **210**, 113–153.
- THOMSON, D. J. & DEVENISH, B. J. 2005 Particle pair separation in kinematic simulations. *J. Fluid Mech.* **526**, 277.
- Wilkinson, M. & Mehlig, B. 2005 Caustics in turbulent aerosols. *Europhys. Lett.* **71** 186–192.
- XU, H., BOURGOIN, M., OUELLETTE, N.T., & BODENSCHATZ, E. 2006 High Order Lagrangian Velocity Statistics in Turbulence. *Phys. Rev. Lett.* **96**, 024503.
- XU, H., PUMIR, A., & BODENSCHATZ, E. 2011 The pirouette effect in Turbulence. *Nature Phys.* **7**, 709–712.
- YAKHOT, V. 2006 Probability densities in strong turbulence. *Physica D* **215** 166.